

## Fractal property of two-dimensional continuum percolation clusters

Mitsunobu Nakamura

*Department of Electronic Engineering, Tamagawa University, Machida, Tokyo 194, Japan*

(Received 24 March 1986)

We have been studying the two-dimensional continuum percolation problem, using patterns on square cellular structures (square meshes) generated by computer simulation. The metallic critical volume fractions for the metal-insulator transition and the effective conductivities of their patterns agreed well with those of actual materials formed by deposition of metal films on insulator substrates. In this paper we obtain the fractal dimensions of percolation clusters of the two-dimensional continuum percolation models formed by computer simulation, and compare the fractal dimensions with the results from the actual experiments of Voss, Laibowitz, and Alessandrini and of Kapitulnik and Deutscher, using transmission electron micrographs of thin metal films deposited on insulator substrates. We clearly show that the fractal properties of percolation clusters on square cellular structures agree well with those of actual experiments. The fractal dimensions are 1.9 for the large percolation clusters occurring when the metallic volume fraction is close to the critical volume fraction for the metal-insulator transition.

### I. INTRODUCTION

One of the methods for treating the continuum percolation (CP) problem is the filling of a lattice space by placing rigid spheres on all the lattice points. Then the metallic critical volume fraction (CVF)  $v_c$  for the metal-insulator transition is presented by<sup>1</sup>

$$v_c = fp_c, \quad (1)$$

where  $p_c$  is the critical site percolation probability of the lattice, and  $f$  is the filling factor, defined as the ratio of the volume of an inscribed sphere to that of a unit cell.<sup>1</sup> The dimensional invariants for the CVF hold for the two-dimensional (2D) and three-dimensional (3D) system as follows:

$$v_c = \begin{cases} 0.45 \pm 0.03 & \text{for 2D,} \\ 0.16 \pm 0.02 & \text{for 3D.} \end{cases} \quad (2)$$

(3)

Using square cellular structures or square meshes instead of lattices, we have been studying the 2D CP.<sup>2-5</sup> In a cellular structure, the flows of percolation are transmitted on cells through the boundaries of a cell not on lattice points and bonds, and the paths of percolation have finite widths. In the CP, the CVF is given by

$$v_c = p_{cc} \quad (4)$$

for the cellular structure with a uniform cell, where  $p_{cc}$  is the critical cellular percolation probability. In our previous paper,<sup>5</sup> hereafter denoted as I, we showed that the CVF of the CP models formed on a square mesh changes from 0 to 1 depending on the method of generation of percolation clusters. As the shapes of deposited metal films are elongated, the CVF becomes close to zero. The dimensional invariant such as (2) does not hold for the 2D CP.

Voss, Laibowitz, and Alessandrini<sup>6,7</sup> presented the CVF

and fractal property of a 2D CP pattern, using transmission electron micrographs of thin gold films deposited on insulator substrates. Their CVF (0.74) agreed well with that (0.73) of one of the CP models in I. In this paper we obtain the fractal dimensions of four types of CP model in I, and compare them with the results from actual experiments by Voss, Laibowitz, and Alessandrini and by Kapitulnik and Deutscher.<sup>8</sup>

Although the problems of the CP appear as often as those of the lattice percolation, fewer results for the frac-

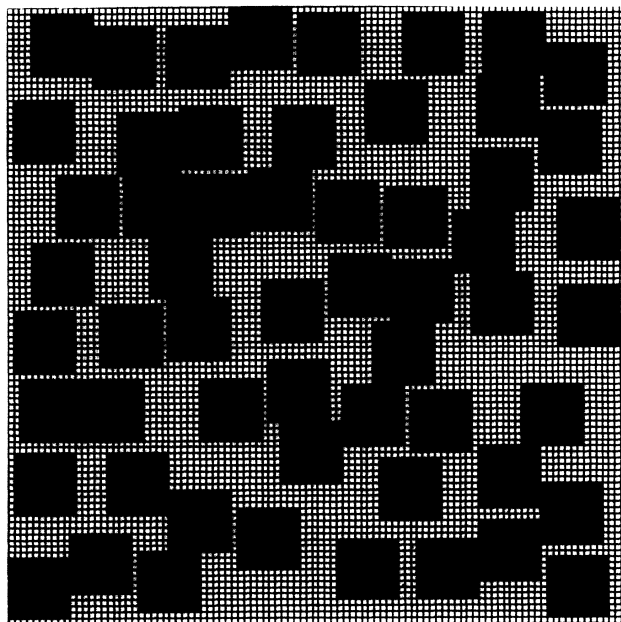


FIG. 1. Two-dimensional continuum percolation pattern formed on a substrate with  $100 \times 100$  unit cells. The black parts whose volume fraction is 0.57 are metals for model *A* and insulators for model *B*.

tal dimension of the CP have been published than those<sup>9-15</sup> of the lattice percolation. With this situation in mind, we discuss here the fractal property of 2D CP, using computer simulation and the results from actual measurements.<sup>6-8</sup>

In Sec. II we present our 2D CP models generated on square meshes by computer simulation. In Sec. III we obtain the fractal dimensions of the models, compare them with previously published results, and discuss the fractal property of the 2D CP.

## II. CONTINUUM PERCOLATION MODELS ON SQUARE CELLULAR STRUCTURES

Here we use four types of 2D CP model formed on square meshes by computer simulation. These four types were already presented in I, but here we again give the four models denoted as *A*, *B*, *C*, and *D*.

We use as substrates or matrices square meshes with  $50 \times 50$ ,  $100 \times 100$ , and  $200 \times 200$  unit meshes or cells. In model *A*, square metal films with  $n \times n$  unit cells are deposited on the meshes of an insulator substrate at random, one by one. In the depositions, any overlap among the deposited films is prohibited, but any contact is permitted. The depositions are repeated, searching places where no overlaps occur, and continued until any square with  $n \times n$  unit cells cannot be placed without any overlap.

In Fig. 1 we present for  $n=10$  one pattern of metal film deposited on an insulator substrate with  $100 \times 100$  unit meshes. The volume fraction of metal (the black

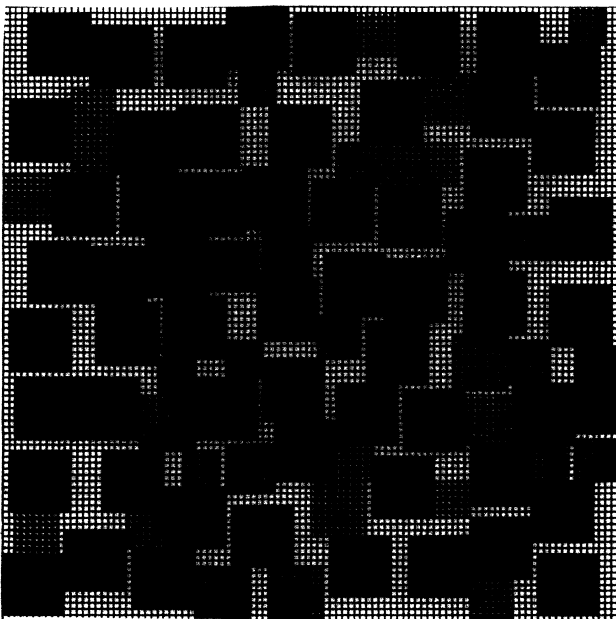


FIG. 2. Pattern further packed in Fig. 1. The shaded squares were deposited into Fig. 1. The volume fraction of the black and shaded portions is 0.7567.

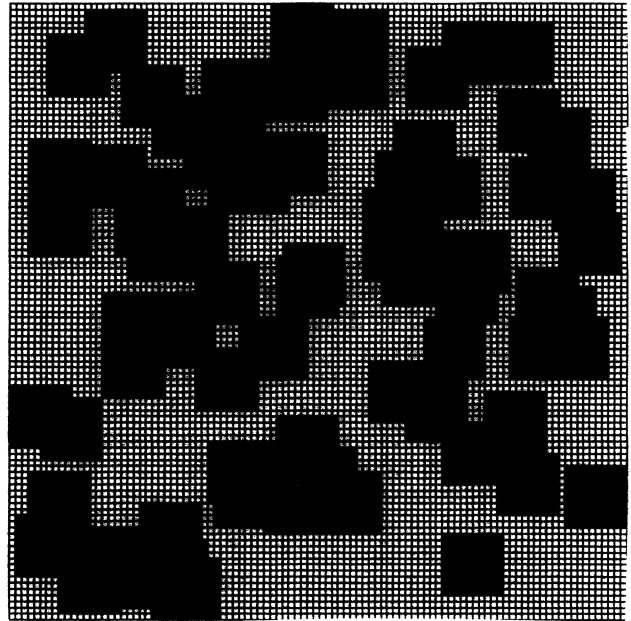


FIG. 3. Two-dimensional continuum percolation pattern. The black parts whose volume fraction is 0.555 are metals for model *C* and insulators for model *D*.

parts) of Fig. 1 is 0.57 and the material is still an insulator because, in fact, the black parts of Fig. 1 are not continuous from one side to the opposite side. To obtain a conductor, we further deposit square metal films with  $9 \times 9$  unit cells in the same manner. The volume fraction becomes unity when square films with  $8 \times 8, 7 \times 7, \dots, 1 \times 1$  unit cell(s) have been deposited in the same method. In Fig. 2 we present one pattern in the course of such operations. The texture in Fig. 2 is obtained by placing squares with  $9 \times 9, 8 \times 8, 7 \times 7$ , and  $6 \times 6$  unit meshes onto the pattern of Fig. 1. The shaded squares in Fig. 2 are newly added in Fig. 1. The metal volume fraction of Fig. 2 is 0.7567 and the texture is a conductor.

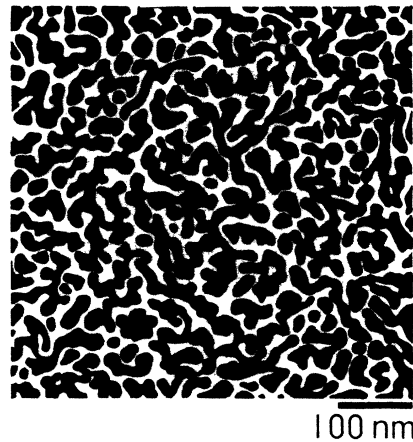


FIG. 4. The pattern of Voss, Laibowitz, and Alessandrini, denoted by VLA, at the volume fraction  $v=0.64$  ( $< v_c=0.74$ ). Gold-film areas are indicated by black.

When the matrices are metals and square holes are punched prohibited overlaps and permitted contacts, the black and shaded portions of Figs. 1 and 2 are insulators. Then the materials are another CP model. We denote by *B* this CP model. Figures 1 and 2 represent either model *A* or *B* depending on whether the black and shaded parts are metals or insulators.

In model *C* the substrates are insulators, but when square metal films are deposited, not only contacts but also overlaps are permitted. When an overlap occurs, the metal film is deposited only on the portion of nonoverlap.

Model *D* is formed by the exchange of metals and insulators in model *C*, just as model *B* is obtained by the exchange of metals and insulators in model *A*. We depict in Fig. 3 one pattern of *C* and *D* for  $n = 10$  shaped on a substrate with  $100 \times 100$  unit cells. When the black portions of Fig. 3 are metals, the texture is model *C*, and when the black parts are insulators, the texture is model *D*. The volume fraction of black parts of Fig. 3 is 0.5505. In Fig. 4 we show one of the patterns of gold films deposited on substrates by Voss, Laibowitz, and Alessandrini (VLA), using transmission electron micrographs. The black parts are gold films and the volume fraction is 0.64 ( $< v_c = 0.74$ ). Hereafter we denote their textures by VLA.

When  $n = 1$ , models *A*, *B*, *C*, and *D* are the same models. As  $n$  increases, the discrepancies among the models become substantial. In I we showed that when  $n \gg 1$  the CVF of model *A* is 0.73 and agrees well with that (0.74) of VLA, and that the CVF of model *D* is 0.42

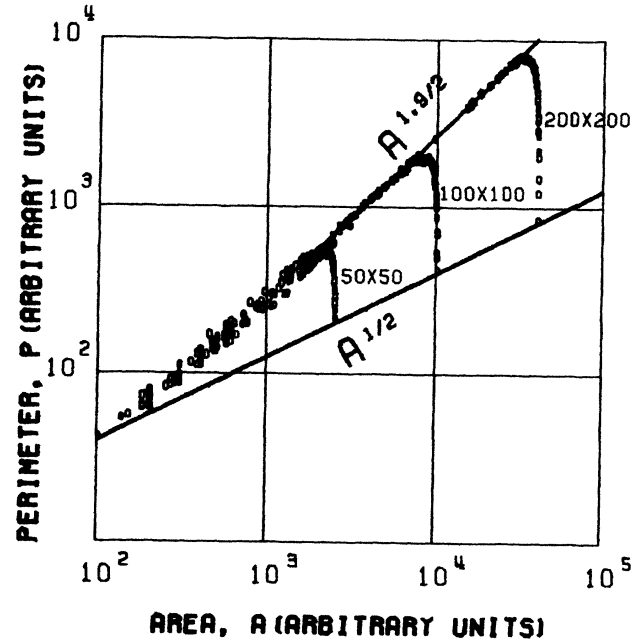


FIG. 5. Scatter plot of the perimeter  $P$  versus area  $A$  for the clusters of model *A*.

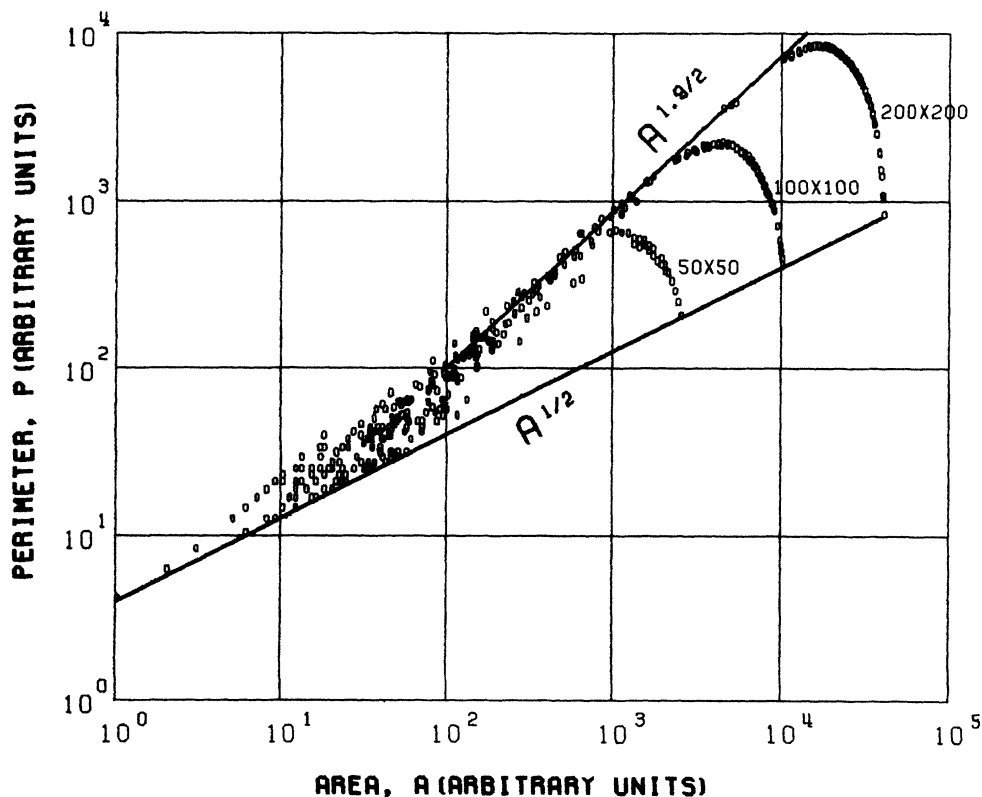


FIG. 6. Scatter plot of the perimeter  $P$  versus area  $A$  for the clusters of model *B*.

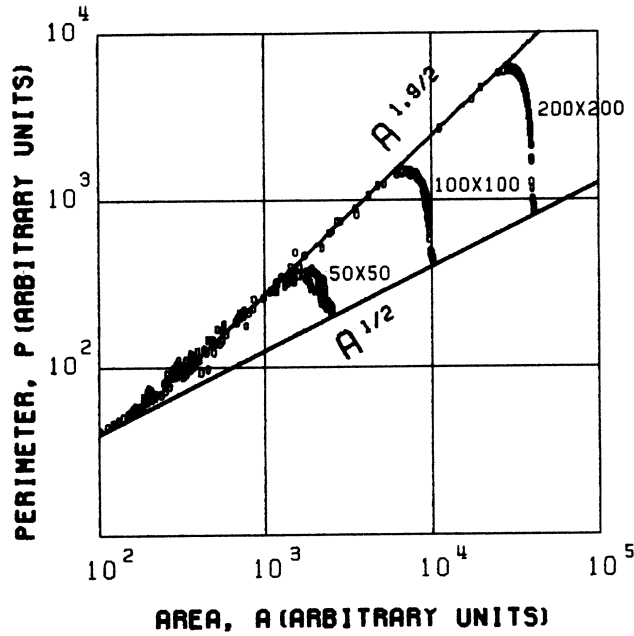


FIG. 7. Scatter plot of the perimeter  $P$  versus area  $A$  for the clusters of model C.

and agrees well with that (0.407) of the experiment of Smith and Lobb.<sup>16</sup> In this paper we use  $n = 10$ .

### III. FRACTAL PROPERTY OF TWO-DIMENSIONAL CONTINUUM PERCOLATION CLUSTERS

The fractal dimension  $D_f$  is defined in many forms.<sup>9</sup> A relation for  $D_f$  of the 2D problem is given by

$$P \propto A^{D_f/2}, \tag{5}$$

where  $P$  is the perimeter of fractal objects and  $A$  is the area. Lovejoy<sup>17</sup> used (5) to estimate the fractal dimension of cloud and rain area boundaries. Voss, Laibowitz, and Alessandrini also applied (5) with other relations. Naturally the fractal dimensions obtained by the different relations were consistent.<sup>6,7</sup> In this paper we also use (5), because in our computer simulation it is easiest and most direct to estimate the relation between  $P$  versus  $A$  of percolation clusters shaped on square meshes.

We plot  $P$  against  $A$  of clusters in Figs. 5, 6, 7, and 8, respectively, for models A, B, C, and D. In Fig. 9 we

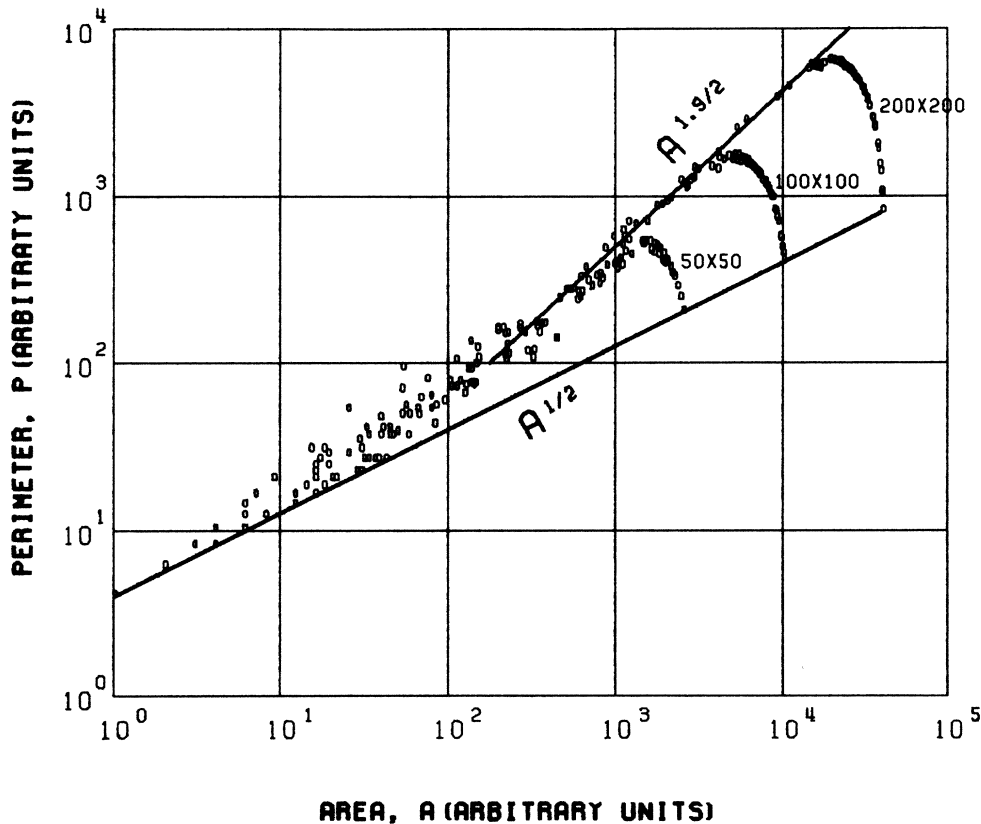


FIG. 8. Scatter plot of the perimeter  $P$  versus area  $A$  for the clusters of model D.

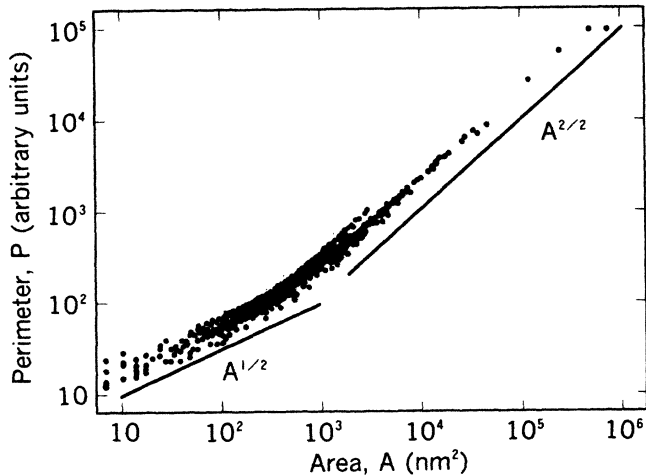


FIG. 9. Scatter plot of the perimeter  $P$  versus area  $A$  for the gold clusters by Voss, Laibowitz, and Alessandrini.

present the same data for VLA. The numbers of unit cells of the substrates are indicated in Figs. 5–8 as  $50 \times 50$ ,  $100 \times 100$ , and  $200 \times 200$ . As shown in Figs. 5–8, there are three stages in the relation between  $A$  and  $P$ . In the first stage where the percolation clusters are small and localized, the data points greatly scatter. In the

second stage where the metallic volume fraction becomes close to the CVF and large clusters occur,  $D_f$  of the large clusters is presented by

$$D_f = 1.9 \quad (6)$$

for all the models. Zallen<sup>18</sup> expressed the clusters of the second stage as “all skin and no flesh,” and in the stage the clusters are skinny. In the third stage where the metallic volume fraction is beyond the CVF, the perimeters of the largest clusters rapidly decrease, the largest clusters again become fleshy,  $D_f$  decreases and at last it becomes unity. These behaviors are obtained in all the four 2D CP models, independently of the numbers of unit cells of the substrates, though the sizes of the largest clusters depend on the numbers.

In the experimental result (Fig. 9) for VLA, the third stage is not shown; however, the behavior of the first and second stages agrees well with those of models  $A$ ,  $B$ ,  $C$ , and  $D$ . The fractal dimensions [Eq. (6)] agree with those of VLA and with those of Kapitulnik and Deutscher,<sup>8</sup> using transmission electron micrographs of Pb films deposited on amorphous Ge. The fractal dimensions also coincide with those of the 2D lattice percolation problem.<sup>9–11</sup>

Finally, we compare in Fig. 10 the data points of the perimeter  $P$  versus area  $A$  for the clusters of models  $A$ ,  $B$ ,

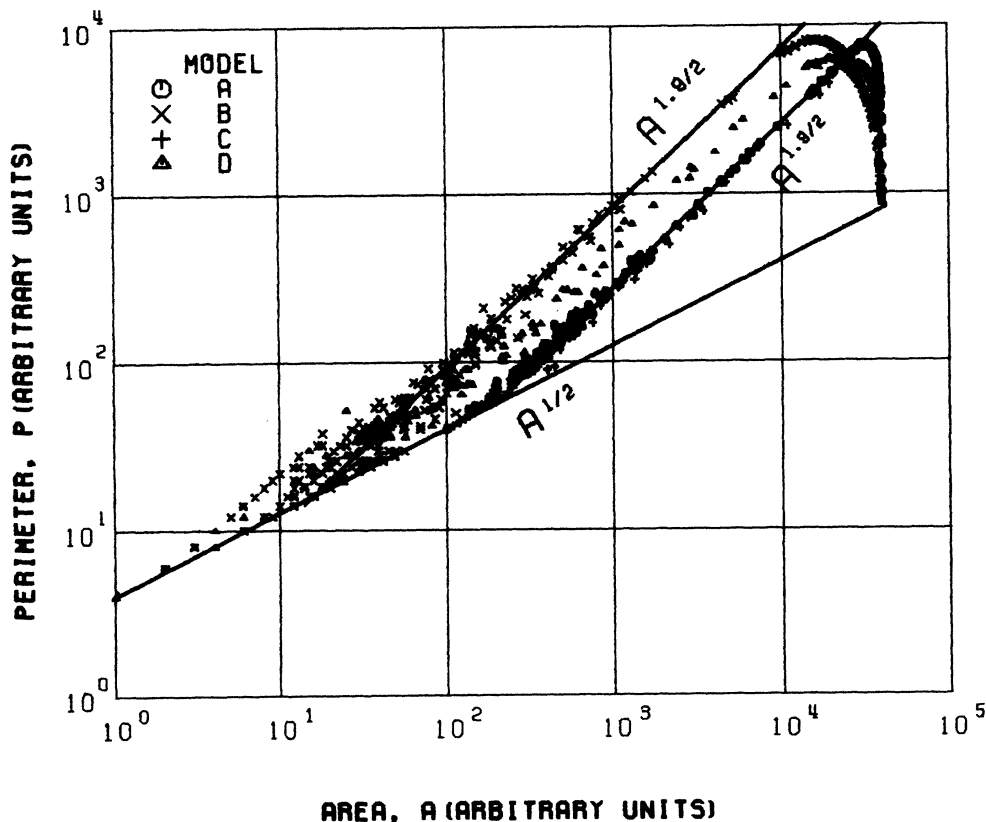


FIG. 10. Scatter plot of the perimeter  $P$  versus area  $A$  for the clusters of models  $A$ ,  $B$ ,  $C$ , and  $D$ , whose substrates have  $200 \times 200$  unit meshes.

$C$ , and  $D$  formed on substrates with  $200 \times 200$  unit cells. The behaviors of  $P$  versus  $A$  for all the four models are very similar to each other, particularly in  $A$  and  $C$ , and in  $B$  and  $D$ .

#### IV. CONCLUSIONS

We have studied the two-dimensional continuum percolation and conduction, using random patterns formed on square cellular structures, and the critical volume fractions for the metal-insulator transition and effective conductivities agreed well with experimental results for metal films deposited on insulator substrates.

In this paper we studied the fractal properties of the random patterns. It was clearly shown that not only the critical volume fractions and effective conductivities but also the fractal properties of the random patterns agree well with experimental results using transmission electron micrographs of metal films deposited on insulator substrates.

The fractal dimension of the models in this paper is 1.9 for the large clusters occurring when the metallic volume fraction is close to the critical volume fraction, and the value agrees well also with that (1.9) of the two-dimensional lattice percolation.

The random patterns shaped on square meshes are not similar in their forms to the metal films deposited on substrates, however, the basic physical properties for the randomness such as critical volume fraction, effective conductivity, and fractal dimension agree well with each other.

#### ACKNOWLEDGMENTS

The author wishes to thank Mrs. Kameko and Dr. Kame for their encouragement and assistance. The formation of patterns and numerical procedures was carried out on the HITAC S-810 and M-280H computers of the University of Tokyo.

<sup>1</sup>V. K. Shante and S. Kirkpatrick, *Adv. Phys.* **20**, 325 (1971).

<sup>2</sup>M. Nakamura and M. Mizuno, *J. Math. Phys.* **23**, 1228 (1982).

<sup>3</sup>M. Nakamura, *J. Appl. Phys.* **56**, 806 (1984).

<sup>4</sup>M. Nakamura, *J. Appl. Phys.* **57**, 1449 (1985).

<sup>5</sup>M. Nakamura, *J. Appl. Phys.* **58**, 3499 (1985).

<sup>6</sup>R. F. Voss, R. B. Laibowitz, and E. I. Alessandrini, *Phys. Rev. Lett.* **49**, 1441 (1982).

<sup>7</sup>R. F. Voss, R. B. Laibowitz, and E. I. Alessandrini, in *The Mathematics and Physics of Disordered Media*, edited by B. D. Hughes and B. W. Ninham (Springer-Verlag, Berlin, 1983), p. 153.

<sup>8</sup>A. Kapitulnik and G. Deutscher, *Phys. Rev. Lett.* **49**, 1444 (1982).

<sup>9</sup>B. B. Mandelbrot, *The Fractal Geometry of Nature* (Freeman, San Francisco, 1983).

<sup>10</sup>D. Stauffer, *Phys. Rep.* **54**, 1 (1979).

<sup>11</sup>Y. Gefen, B. B. Mandelbrot, and A. Aharony, *Phys. Rev. Lett.* **45**, 855 (1980).

<sup>12</sup>Y. Gefen, A. Aharony, B. B. Mandelbrot, and S. Kirkpatrick, *Phys. Rev. Lett.* **47**, 1771 (1981).

<sup>13</sup>P. L. Leath and G. R. Reich, *J. Phys. C* **11**, 4017 (1978).

<sup>14</sup>P. L. Leath, *Phys. Rev. B* **14**, 5046 (1976).

<sup>15</sup>S. Kirkpatrick, in *Ill-Condensed Matter*, edited by R. Balian, R. Maynard, and G. Toulouse (North-Holland/World Scientific, Amsterdam, 1979), p. 324.

<sup>16</sup>L. N. Smith and C. J. Lobb, *Phys. Rev. B* **20**, 3653 (1979).

<sup>17</sup>S. Lovejoy, *Science* **216**, 185 (1982).

<sup>18</sup>R. Zallen, *The Physics of Amorphous Solids* (Wiley, New York, 1983).

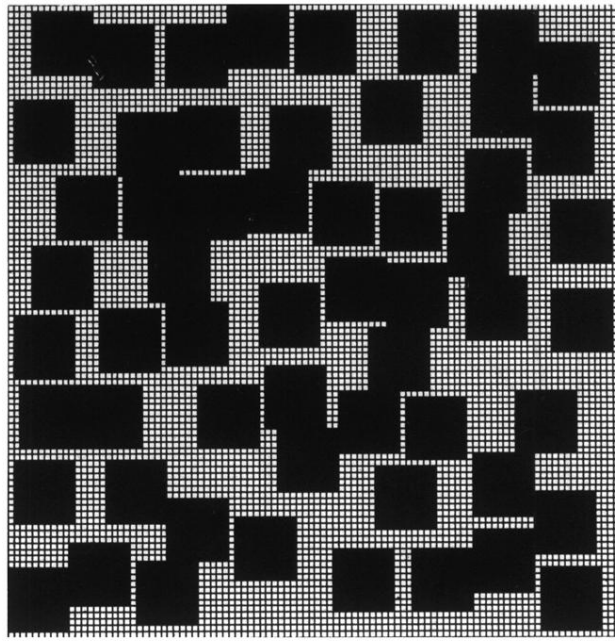


FIG. 1. Two-dimensional continuum percolation pattern formed on a substrate with  $100 \times 100$  unit cells. The black parts whose volume fraction is 0.57 are metals for model *A* and insulators for model *B*.

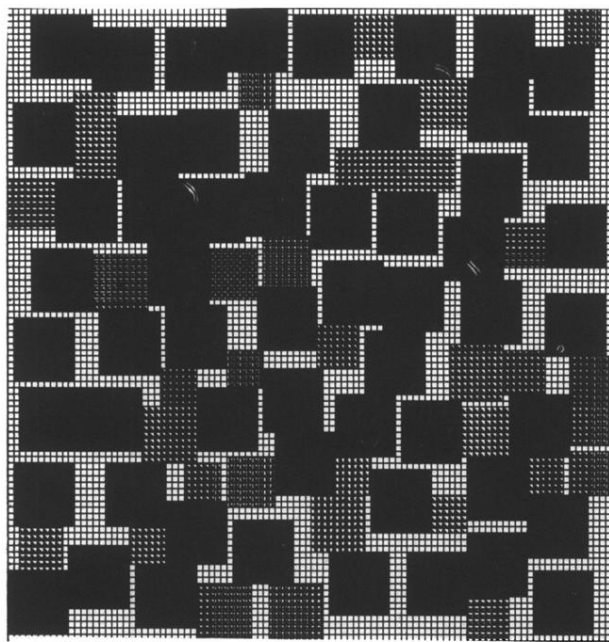


FIG. 2. Pattern further packed in Fig. 1. The shaded squares were deposited into Fig. 1. The volume fraction of the black and shaded parts is 0.7567.



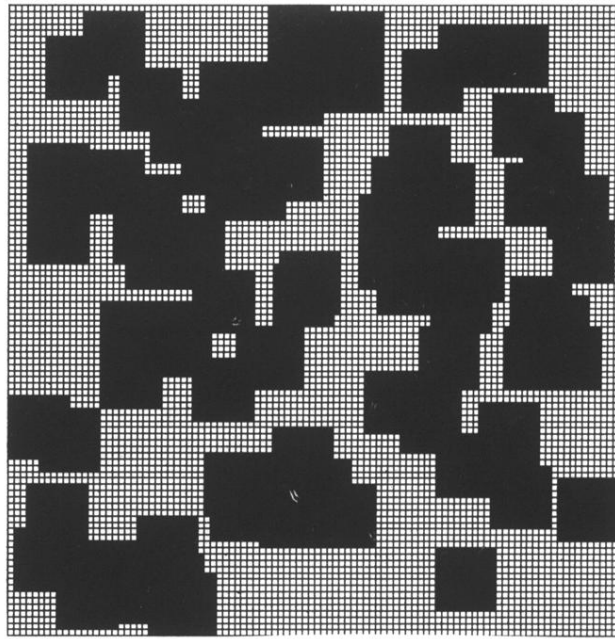
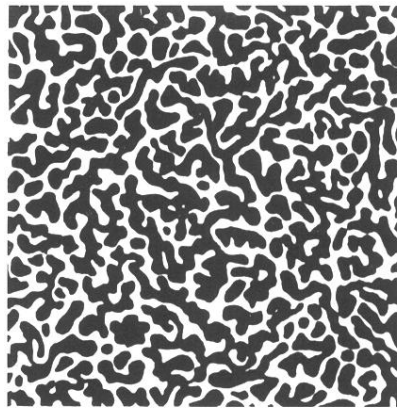


FIG. 3. Two-dimensional continuum percolation pattern. The black parts whose volume fraction is 0.555 are metals for model *C* and insulators for model *D*.



100 nm

FIG. 4. The pattern of Voss, Laibowitz, and Alessandrini, denoted by VLA, at the volume fraction  $v = 0.64$  ( $< v_c = 0.74$ ). Gold-film areas are indicated by black.